Quantitative Systems Toxicology Predicts Ivacaftor-Induced Oxidative Stress Contributes to CFTR Modulator Hepatotoxicity

Alan Shi[1], Cole Cornwell[1], Kyunghee Yang[2] and Paul M. Beringer[1,3,*]

Cystic fibrosis (CF) is a chronic hereditary disease that affects tens of thousands of people worldwide. The introduction of CFTR modulator therapies such as elexacaftor/tezacaftor/ivacaftor (ETI) has significantly improved the quality of life of people with CF. However, ETI has been shown in clinical trials to cause elevations in liver enzymes, and real-world cases of drug-induced liver injury (DILI) have also been reported. The mechanism of ETI-mediated DILI is currently unknown, hindering the development of more effective mitigation strategies for this adverse reaction. Through *in vitro* assays and quantitative systems toxicology modeling using DILIsym, this study revealed that ivacaftor contributed most significantly to ETI-mediated DILI, primarily via reactive oxygen species production, resulting in mitochondrial dysfunction due to electron transport chain inhibition. DILIsym modeling also predicted liver enzyme elevations following daily dosing of ETI at a comparable frequency (6.0%) to that of clinical data (8.0%). Simulations of the therapeutic effects of DILI mitigation strategies for ETI showed that dose reduction and antioxidant administration may significantly reduce the frequency of liver enzyme elevations due to ETI.

Study Highlights

WHAT IS THE CURRENT KNOWLEDGE ON THE TOPIC?

☑ Elexacaftor/tezacaftor/ivacaftor, a highly effective CFTR modulator therapy, has been observed in clinical trials and case reports to cause liver enzyme elevations and drug-induced liver injury (DILI). However, the mechanism(s) of ETI-mediated DILI are unknown, making it difficult to identify an optimal treatment strategy to mitigate this potentially severe adverse reaction.

WHAT QUESTION DID THIS STUDY ADDRESS?

☑ This study incorporated *in vitro* hepatotoxicity assays and quantitative systems toxicology (QST) modeling to understand the mechanistic basis of ETI-mediated DILI, simulate DILI biomarker levels, and predict the therapeutic benefits of ETI dose reduction or experimental antioxidant treatments.

WHAT DOES THIS STUDY ADD TO OUR KNOWLEDGE?

☑ *In vitro* assays and modeling identified the major mechanism of ETI-mediated DILI (oxidative stress due to ivacaftor). The predicted decrease in the frequency of liver enzyme elevations due to dose reduction and antioxidant therapies supports their use as mitigation strategies for ETI-mediated DILI.

HOW MIGHT THIS CHANGE CLINICAL PHARMACOLOGY OR TRANSLATIONAL SCIENCE?

☑ Our study shows how *in vitro* mechanistic assays coupled with QST modeling can be used to reveal the DILI mechanisms of approved drugs and forecast the impact of DILI mitigation strategies, which can directly improve management of DILI in the clinic.

Cystic fibrosis is a serious chronic illness caused by mutations to the cystic fibrosis transmembrane conductance regulator (CFTR) protein, and it affects ~89,000 people worldwide. Clinical manifestations of CF include airway obstruction, inflammation, increased lung infection risk, pancreatic insufficiency, diabetes, and nutrient malabsorption.[1] Improvements in treatments for CF over time have resulted in significantly improved median predicted survival for people with CF in the United States, from 30 years among those born 1990–1994 to 53 years among those born 2017–2021.[2]

Elexacaftor/tezacaftor/ivacaftor (ETI) is a highly effective CFTR modulator therapy for cystic fibrosis. In clinical trials, ETI has significantly improved both lung function and nutritional status in people with cystic fibrosis.[3] ETI is generally well tolerated with few safety concerns; however, drug-induced liver injury (DILI), a rare but potentially life-threatening adverse reaction, has been identified in clinical trials and post-marketing reports.[3–11] Our group also confirmed the statistically significant disproportionate association between ETI and DILI on a larger scale by conducting a pharmacovigilance analysis of

[1]Department of Clinical Pharmacy, Mann School of Pharmacy and Pharmaceutical Sciences, University of Southern California, Los Angeles, California, USA; [2]Quantitative Systems Pharmacology Solutions, Simulations Plus Inc., Research Triangle Park, North Carolina, USA; [3]USC Anton Yelchin CF Clinic, Los Angeles, California, USA. *Correspondence: Paul M. Beringer (beringer@usc.edu)

Received May 9, 2025; accepted September 9, 2025. doi:10.1002/cpt.70073

adverse event reports in the FDA adverse event reporting system (FAERS) database.[12]

DILI is an adverse drug reaction caused by medication-induced damage to the liver. The clinical presentation of DILI may involve one or more of the following symptoms: fatigue, nausea, malaise, pruritus, fever, rash, and jaundice.[13] Diagnosis of DILI involves assessing the temporal relationship between drug exposure, confounding risk factors, and the development of signs and symptoms of liver disease.[13] Outcomes for DILI range from complete resolution to hospitalization, acute liver failure requiring transplantation, and death (at roughly 10% of patients for highly toxic drugs).[13,14] Criteria for treatment discontinuation are based on elevation of liver enzymes: alanine aminotransferase (ALT) > 8× upper limit of normal (ULN), ALT > 5× ULN for 3 weeks, ALT > 3× ULN + total bilirubin > 2× ULN, prothrombin time (PT)–international normalized ratio (INR) > 1.5× ULN or in the presence of symptoms suggesting liver injury.[13,15] Major mechanisms for DILI include mitochondrial toxicity, oxidative stress, and disruption of bile acid transport in the liver.[14] DILI is one of the most common causes of drug failure in clinical development and a major cause of drug withdrawal from the market because of pharmacovigilance findings in the post-marketing phase.[14]

Despite accumulating evidence of DILI from clinical trials, real-world case reports, and pharmacovigilance analysis, a clear mechanistic basis of ETI-mediated DILI is not known.[16] Because treatment discontinuation of ETI due to DILI would have a devastating effect on the quality of life of people with CF, understanding the mechanism of ETI-mediated DILI is urgently needed to identify potential interventions (e.g., emerging biomarkers, dose adjustments, and therapeutic compounds) to mitigate DILI.

For drugs removed from the market due to DILI, preclinical testing in animal models has poorly predicted the occurrence of DILI in humans, likely due to species-specific differences in drug metabolism pathways.[17,18] However, the mechanistic assessment of reference hepatotoxic drugs using human-derived *in vitro* models coupled with quantitative systems toxicology (QST) has been demonstrated to accurately predict the DILI potential of new compounds.[19–28] QST models such as DILIsym incorporate pharmacokinetic variability, patient susceptibility factors, and *in vitro* mechanistic data to simulate liver toxicity and predict DILI in a simulated population with inter-individual variability in susceptibility to liver injury.[20,25] This approach provides the ideal framework for post-marketing exploration of the DILI mechanisms of ETI and for optimizing the dosing protocol to mitigate DILI.

This study aimed to determine the mechanism of ETI-mediated DILI through *in vitro* hepatocyte assays and QST modeling of the *in vitro* data. Furthermore, QST modeling was used to determine the relative contribution of each mechanism and each ETI compound to DILI, evaluate potential emerging biomarkers for DILI, and predict the efficacy of therapeutic strategies for DILI such as dose reduction or coadministration of mechanism-targeting therapeutic compounds.

METHODS

In vitro mechanistic assays

ETI hepatotoxicity was assessed in *in vitro* assays corresponding to the three major mechanisms of hepatotoxicity represented in DILIsym: mitochondrial dysfunction, oxidative stress, and bile acid transporter inhibition. A deuterated analog of ivacaftor has recently been approved by the FDA as part of a triple-combination CFTR modulator therapy vanzacaftor/tezacaftor/deutivacaftor.[29] The hepatotoxicity of this deuterated ivacaftor (deutivacaftor, D9 Iva) was also assessed *in vitro*. Intracellular concentrations of ETI in mitochondrial dysfunction and oxidative stress assays were estimated using physiologically-based pharmacokinetic (PBPK) modeling of the liver:blood exposure ratio (liver:blood Kp) in Simcyp. Steady-state plasma and liver C_{max} levels for ETI parent compounds were predicted using our previously validated PBPK model of ETI.[30] For ETI primary metabolites (M23 elexacaftor, M1 tezacaftor, M1 ivacaftor), the plasma and liver C_{max} values were scaled from the predicted values for the parent compounds based on published steady-state AUC values of ETI parent compounds and metabolites.[31,32]

Mitochondrial dysfunction. Cellular respiration assays were conducted in HepG2 cells using the Seahorse XFe96 (Agilent Technologies, CA) after a 1-hour incubation with each ETI compound, metabolite, and deutivacaftor following the Seahorse Mito Stress Test Kit protocol.[33] The resulting baseline oxygen consumption rate (OCR) measurement was analyzed as the fold change of each ETI compound/metabolite compared with the negative control (0.2% DMSO vehicle). Ciglitazone was used as a positive control, as it was previously shown to significantly impair mitochondrial function.[34] The nominal concentration range for each compound encompassed their predicted plasma C_{max} and liver C_{max} values.

Oxidative stress. In accordance with a previous study by Longo *et al.*,[35] oxidative stress assays were conducted in HepG2 cells using the Cytation 5 high-content imager after a 1-hour and 24-hour incubation with each ETI compound, metabolite, and deutivacaftor, followed by a 30-minute incubation with dihydroethidium (DHE), a fluorescent probe for reactive oxygen species (ROS). The measured fluorescence intensity of DHE was analyzed as the fold change of each ETI compound/metabolite compared with the negative control (0.2% DMSO vehicle). Troglitazone, a known inducer of ROS,[36] was used as a positive control. The nominal concentration range for each compound encompassed their predicted plasma C_{max} and liver C_{max} values.

Bile acid transporter inhibition. ETI-induced BSEP inhibition was assessed in HEK293 human BSEP vesicles using a taurocholate uptake (BSEP substrate) assay with cyclosporin A as a positive control (Pharmaron, Waltham, MA). ATP-dependent uptake activity was calculated after measuring intracellular taurocholate in the presence/absence of ATP via LCMS/MS and was analyzed as the percentage of vehicle control (DMSO) activity.

In silico modeling

DILIsym is a mathematical and mechanistic model of DILI that takes inputs from *in vitro* hepatotoxicity data, PBPK predictions of drug concentration-time data, and built-in simulated human populations (SimPops) to simulate the occurrence of liver injury for a given compound or compounds.[37] DILIsym version 10 (DSX) was used for all simulations described in this manuscript.

Translation into DILIsym parameters. The *in vitro* results for each of the three mechanisms (mitochondrial dysfunction, oxidative stress, and bile acid transport inhibition) were translated into DILIsym

input parameters used in conducting simulations of liver injury due to ETI. MITOsym, a companion program of DILIsym incorporating a mechanistic model of *in vitro* hepatocellular respiration, was used to derive parameter values for ETI-mediated mitochondrial dysfunction.[38] The OCR-concentration data for elexacaftor and ivacaftor was reproduced in MITOsym simulations through a sensitivity analysis approach to obtain the ETC inhibition parameters resulting from in OCR predictions that most closely matched the observed *in vitro* data. The mitochondrial dysfunction parameters from MITOsym were converted to DILIsym input parameters using previously established scaling factors, which were derived from exemplar compounds known to cause mitochondrial toxicity—specifically, rotenone (ETC inhibition), FCCP (uncoupling), and oligomycin (ATP synthase inhibition).[35,38] For oxidative stress, ROS-concentration data for elexacaftor and ivacaftor was predicted using DILIsym through a similar sensitivity analysis process; the ROS production rate constants that most closely matched observed *in vitro* data were used as DILIsym input parameters. For bile acid transporter inhibition, the BSEP IC_{50} value for elexacaftor was directly entered into DILIsym as the inhibition constant. Since elexacaftor, tezacaftor, and ivacaftor are not known to be substrates or modulators of other hepatic transporters (e.g., NTCP), we have chosen to include only BSEP in our DILI model. Tezacaftor and ETI metabolites were not included in the DILIsym model because they did not achieve significant levels of OCR reduction, ROS production, or bile acid transporter inhibition in the physiologically relevant range of plasma C_{max} to liver C_{max}.

PBPK modeling. Plasma and liver concentrations were simulated using validated Simcyp PBPK models of elexacaftor and ivacaftor.[30] Specifically, ivacaftor exposure was simulated at 150 mg twice daily and elexacaftor exposure was simulated at 200 mg daily under high-fat fed conditions for a dosing period of 24 weeks, matching that of a Phase III clinical trial for ETI.[5] The plasma and liver concentration-time profiles were imported into DILIsym using the Specify Data function.

SimPops. DILIsym contains built-in simulated human populations that incorporate variability in biochemical and physical parameters. For this study, the normal healthy volunteer SimPops (Human_ROS_apop_mito_BA_v8A_1, $n = 285$) included in DILIsym X were used. This SimPops includes variability in oxidative stress, caspase activation (apoptosis), mitochondrial function, and bile acid transporter expression. Additionally, mitochondrial biogenesis, an adaptive mechanism by which cells produce mitochondria in response to environmental stressors or developmental signals,[39] was turned on for the simulations to better characterize the observed DILI in clinical trials.

Simulations. Simulations were performed for ivacaftor and elexacaftor, both alone and in combination, in accordance with a previous study assessing the liver effects of cannabidiol and valproate.[40] The software can accommodate up to three drugs in total simultaneously. Ivacaftor and elexacaftor were chosen as the compounds for the ETI model because tezacaftor did not show significant toxicity within its predicted physiological range (plasma C_{max} to liver C_{max}).

To accommodate simulating two compounds simultaneously, the translated DILIsym parameters for ivacaftor were input under the Compound Y model scaffold and the parameters for elexacaftor were input under the Compound X model scaffold (**Table S1**). All simulations were performed sequentially using the $n = 285$ Human_ROS_apop_mito_BA_v8A_1 SimPops with a high-fat diet.

The following simulations were conducted (**Table 1**): standard dose elexacaftor (200 mg/day) and ivacaftor (150 mg twice daily) in combination with sequential omission of individual DILI mechanisms (ROS production, ETC inhibition, BSEP inhibition) (Rows 1–3), standard dose of elexacaftor or ivacaftor alone vs. both compounds in combination (Rows 4–6). Additional simulations were performed to assess the therapeutic effects of ETI dose reduction (Row 7) or the effects of hypothetical antioxidant therapy (Row 8). For dose reduction, the simulation included ivacaftor and elexacaftor in combination with their doses set to half (150 mg daily and 100 mg daily, respectively) with all hepatotoxicity mechanisms on. For the effects of antioxidant therapy, ivacaftor and elexacaftor in combination were set at standard doses (150 mg twice daily and elexacaftor 200 mg daily) with all hepatotoxicity mechanisms on, while the ROS production rate constants in DILIsym were adjusted proportionally to reflect the impact of antioxidant administration on levels of glutathione (GSH, an endogenous ROS scavenger). In *in vivo* studies, intravenous administration of n-acetyl cysteine (NAC) in rats resulted in a 50% increase in levels of GSH in the liver, while intravenous administration of NAC in mice after a toxic dose of acetaminophen resulted in a 75% recovery of liver GSH and a 45% recovery of mitochondrial GSH compared with untreated values.[41,42] Since an increase in ROS-scavenging GSH would correspond to a decrease in ROS levels, the ROS production rate constant 1 and ROS production Vmax 4 were reduced to 50% for the antioxidant effect simulation to approximate the *in vivo* effect of GSH.

RESULTS

In vitro mechanistic assays

Among the three components of ETI, ivacaftor was found to be the most toxic for both oxidative stress and mitochondrial dysfunction, with significant toxicity occurring at physiological levels (between the predicted plasma C_{max}, 2.8 μM, and predicted liver C_{max}, 69.9 μM). All physiological ranges described in this study are between the predicted plasma C_{max} and predicted liver C_{max} of their respective compounds.

Oxidative stress. The ETI parent compounds elexacaftor, tezacaftor, and ivacaftor induced concentration-dependent increases in ROS, but only ivacaftor had significant increases within the predicted physiological range. Elexacaftor induced significant increases in ROS at 40 μM (physiological range 12.1–17.2 μM) (**Figure 1a**). Tezacaftor induced significant increases in ROS at 40 and 80 μM (physiological range 11.3–14.2 μM) (**Figure 1b**). Ivacaftor induced significant ROS increases at 10 and 25 μM, within the predicted physiological range (2.8–69.9 μM). Additionally, the magnitude of ROS increases due to ivacaftor matched or surpassed that of the positive control, troglitazone (**Figure 1c**). Deutivacaftor induced nearly identical levels of ROS increases at the same concentrations as ivacaftor (**Figure S1**). Note: the results described reflect the ROS data from the 24-hour assay, as there were no significant increases in ROS for the 1-hour assay.

The ETI primary metabolites M23 elexacaftor, M1 tezacaftor, and M1 ivacaftor also induced concentration-dependent increases in ROS; however, the effects occurred at concentrations that are predicted to exceed their physiological ranges or were not greater than that of the positive control. Like its parent compound, M23 elexacaftor induced significant increases in ROS at 40 and 80 μM (physiological range 4–5.8 μM) (**Figure 1d**). M1 tezacaftor induced significant increases in ROS at 20, 40, and 80 μM (predicted physiological range 11.5–14.5 μM) (**Figure 1e**). Unlike its parent compound, M1 ivacaftor only induced a significant ROS increase

Table 1 ETI DILI simulation results

Row	Compound(s)	Dose	Mechanisms ON	Mechanisms OFF	Simulated ALT >3× ULN	Simulated Bilirubin >2× ULN	Simulated Hy's Law
1	Ivacaftor and elexacaftor	Standard (Iva 200 mg daily / Elx 100 mg daily)	ETC inhibition, BSEP inhibition	ROS production	0/285	0/285	0/285
2	Ivacaftor and elexacaftor	Standard	ROS production, BSEP inhibition	ETC inhibition	17/285	0/285	0/285
3	Ivacaftor and elexacaftor	Standard	ROS production, ETC inhibition	BSEP inhibition	17/285	0/285	0/285
4	Ivacaftor	Standard	ROS production, ETC inhibition, BSEP inhibition	None	14/285	0/285	0/285
5	Elexacaftor	Standard	ROS production, ETC inhibition, BSEP inhibition	None	0/285	0/285	0/285
6	Ivacaftor and elexacaftor	Standard	ROS production, ETC inhibition, BSEP inhibition	None	17/285	0/285	0/285
7	Ivacaftor and elexacaftor	Half (Iva 100 mg daily / Elx 50 mg daily)	ROS production, ETC inhibition, BSEP inhibition	None	0/285	0/285	0/285
8	Ivacaftor and elexacaftor	Standard	ROS production (50% reduction in ROS rate constant 1 and Vmax 4), ETC inhibition, BSEP inhibition	None	0/285	0/285	0/285

The following simulations were conducted: elexacaftor and ivacaftor in combination with sequential omission of DILI mechanisms (Rows 1–3), administration of elexacaftor or ivacaftor alone vs. both compounds in combination (Rows 4–6), dose reduction of elexacaftor and ivacaftor in combination (Row 7), and elexacaftor and ivacaftor in combination with hypothetical antioxidant coadministration (Row 8).

at 100 µM (predicted physiological range 14.4–359.3 µM), and with a lower level of ROS compared with that of troglitazone (**Figure 1f**).

Mitochondrial dysfunction. Among ETI parent compounds, elexacaftor and tezacaftor induced less pronounced decreases in OCR compared with ivacaftor. Elexacaftor induced a decrease in OCR within the predicted physiological range (12.1–17.2 µM) and more notable decreases at 30 µM and beyond, yielding an IC_{50} of 21.71 µM (**Figure 2a**). Tezacaftor did not induce a notable decrease in OCR within physiological concentrations (11.3–14.2 µM) (**Figure 2b**). Ivacaftor induced the most prominent decrease in OCR within the predicted physiological range (2.8–69.9 µM), with a ~50% decrease at 10 µM and yielding an IC_{50} of 10.33 µM, more potent than that of ciglitazone (~50–100 µM) (**Figure 2c**). Deutivacaftor induced a similar ~50% decrease at 10 µM and an IC_{50} of 11.05 µM (**Figure S1**).

Across the ETI primary metabolites, M23 elexacaftor induced a greater decrease in OCR at physiological concentrations than either M1 tezacaftor or M1 ivacaftor. M23 elexacaftor yielded an IC_{50} of 4.74 µM, more potent than that of its parent compound (IC_{50} of 21.71 µM) and ciglitazone but has a relatively flat inhibition curve compared with its parent compound, with only a small decrease in OCR of less than 20% within its predicted physiological range (4.0–5.8 µM) (**Figure 2d**). M1 tezacaftor, like its parent compound, did not induce a notable decrease in OCR within physiological concentrations

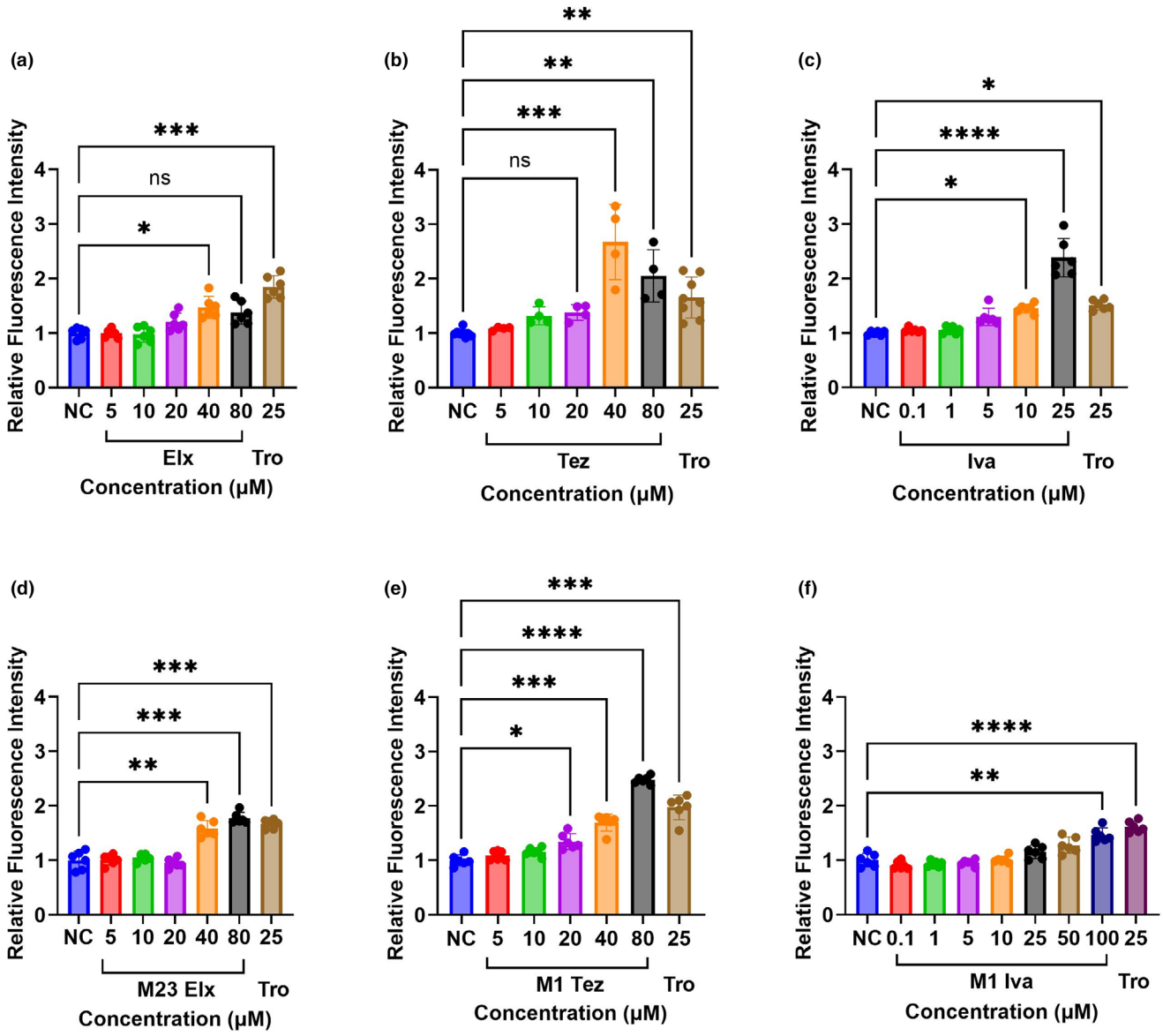

Figure 1 Relative change in reactive oxygen species (represented by dihydroethidium fluorescence intensity) measured by the Cytation 5 high-content imager for the ETI parent compounds (**a**) elexacaftor (Elx), (**b**) tezacaftor (Tez), and (**c**) ivacaftor (Iva), and metabolites (**d**) M23 elexacaftor, (**e**) M1 tezacaftor, and (**f**) M1 ivacaftor. Troglitazone (Tro) was used as the positive control and 0.2% DMSO was used as the negative control (NC). Error bars represent standard deviation. Significant differences between treatment conditions were determined by the Kruskal–Wallis test. *$P<0.05$, **$P<0.01$, ***$P<0.001$, ****$P<0.0001$.

(11.5–14.5 μM) (Figure 2e). M1 ivacaftor also did not induce any notable decrease within the predicted physiological range (14.4–359.3 μM) (Figure 2f).

Bile acid transporter inhibition. Elexacaftor was the most potent BSEP inhibitor among all ETI compounds; however, its IC_{50} of 37.05 μM (95% CI: 15.63–87.83 μM) exceeds its predicted physiological range (predicted plasma C_{max}, 12.1 μM, to predicted liver C_{max}, 17.2 μM) and is less potent than that of the positive control, cyclosporin A (IC_{50} of 1.98 μM, 95% CI: 1.74–2.26 μM) (Figure 3). In contrast, ivacaftor and tezacaftor both yielded a BSEP $IC_{50} > 100$ μM. (Ivacaftor and tezacaftor were omitted from Figure 3 due to their high BSEP IC_{50} values, which were not physiologically relevant.)

In silico modeling

Simulations. Ivacaftor and elexacaftor were chosen as the compounds from ETI used to build the DILI model within DILIsym. Ivacaftor was the most hepatotoxic compound within predicted physiological concentrations from the *in vitro* assays for mitochondrial dysfunction and oxidative stress. Though elexacaftor was not a significant inhibitor of BSEP at predicted physiological concentrations, its BSEP IC_{50} was included in the

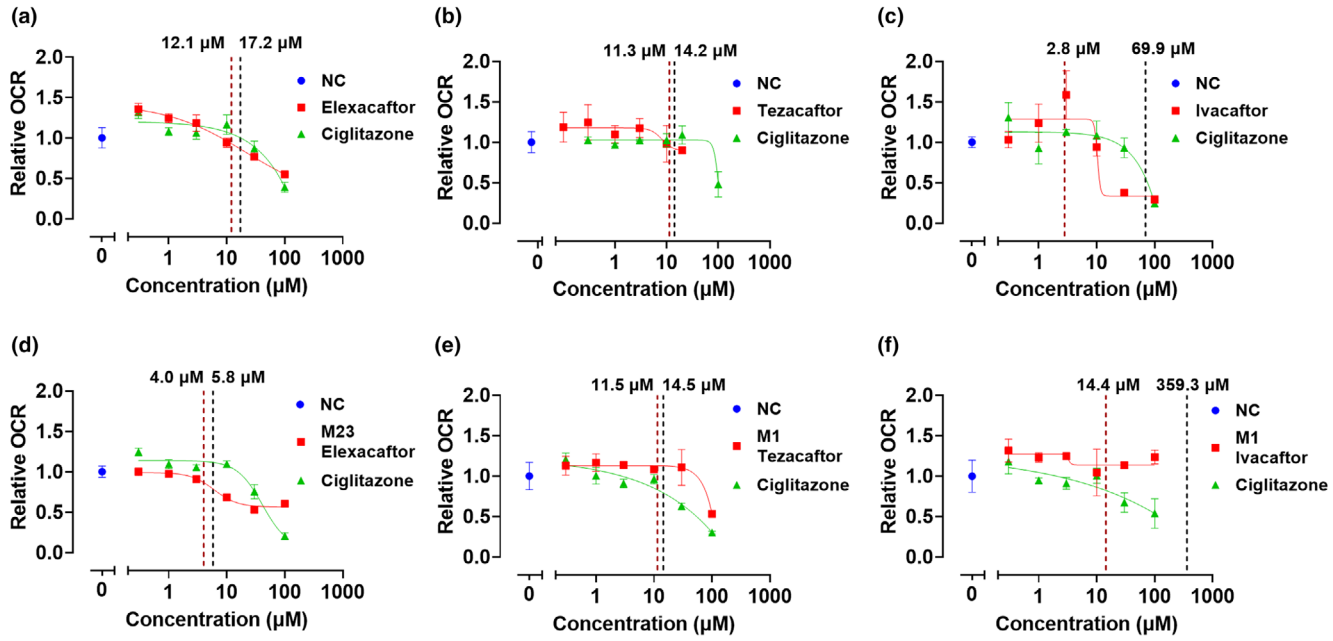

Figure 2 Relative change in oxygen consumption rate measured by the Seahorse XFe96 bioanalyzer for the ETI parent compounds (**a**) elexacaftor, (**b**) tezacaftor, and (**c**) ivacaftor, and metabolites (**d**) M23 elexacaftor, (**e**) M1 tezacaftor, and (**f**) M1 ivacaftor. Concentrations of 0.3, 1, 3, 10, 30, and 100 µM were used for all compounds and the positive control, cigilitazone, except for tezacaftor, (0.1, 0.3, 1, 3, 10, and 20 µM). Parent compounds and metabolites are represented by solid red squares, the negative control (0.2% DMSO) is represented by solid blue circles, and the positive control is represented by solid green triangles. Error bars represent standard deviation. Vertical dashed lines represented predicted physiological range from plasma C_{max} (in red) to liver C_{max} (in black). Best-fit lines were determined by a 4-parameter logistic model.

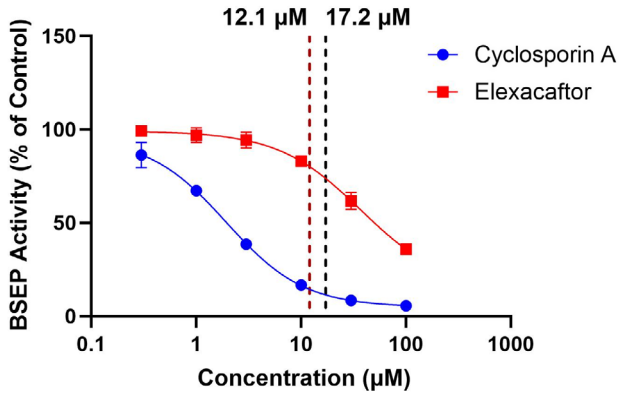

Figure 3 Inhibition of BSEP transporter by elexacaftor compared with the positive control, cyclosporin A, at concentrations of 0.3, 1, 3, 10, 30, and 100 µM. The IC_{50} of elexacaftor was 37.05 µM (95% CI: 15.63–87.83 µM), while the IC_{50} for ivacaftor and tezacaftor were both greater than 100 µM. The IC_{50} of the positive control, cyclosporin A was 1.98 µM (95% CI: 1.74–2.26 µM). Ivacaftor and tezacaftor are not shown because they did not have significant inhibition of BSEP below 100 µM. Vertical dashed lines represented predicted physiological range from plasma C_{max} (in red) to liver C_{max} (in black).

model to assess the contribution of BSEP inhibition to ETI DILI. The calculated DILIsym input parameters for the ETI model are included in **Table S1**.

In simulations of relative mechanistic contribution to DILI, oxidative stress was predicted to be the main driver of ETI hepatotoxicity. The $n = 285$ SimPops dosed with both ivacaftor and elexacaftor with oxidative stress (ROS production rate constants) turned off resulted in a 0% (0/285) predicted occurrence of ALT elevations > 3× ULN or bilirubin > 2× ULN (**Table 1**). In comparison, the SimPops dosed with both ivacaftor and elexacaftor with either ETC inhibition coefficients turned off or BSEP inhibition turned off resulted in a 6.0% (17/285) predicted occurrence of significant LFT elevations, revealing that ETC inhibition and BSEP inhibition have a minimal predicted impact on hepatotoxicity of ETI (**Table 1**).

In simulations of ivacaftor and elexacaftor alone vs. in combination, an increased hepatotoxic effect with the combination was predicted. The $n = 285$ SimPops dosed with ivacaftor alone resulted in a 4.9% (14/285) predicted occurrence of ALT elevations > 3× ULN or bilirubin > 2× ULN, and the SimPops dosed with elexacaftor alone resulted in a 0% (0/285) predicted occurrence of significant LFT elevations, while the SimPops dosed with both ivacaftor and elexacaftor resulted in a greater 6.0% (17/285) predicted occurrence of DILI (**Table 1**). The greater predicted occurrence of DILI for ivacaftor alone vs. elexacaftor alone also corroborates with the results from our *in vitro* investigations, where ivacaftor was found to be the most hepatotoxic of the three ETI compounds.

Predicted time course data for ALT showed a maximal concentration peak at a~ 500 hours (21 days) with a slow decline afterward, which was relatively consistent across the different simulation conditions to predict DILI occurrence (ivacaftor alone, elexacaftor alone, ivacaftor, and elexacaftor in combination) (**Figure 4a**). Predicted levels of AST were about half of those of ALT while still

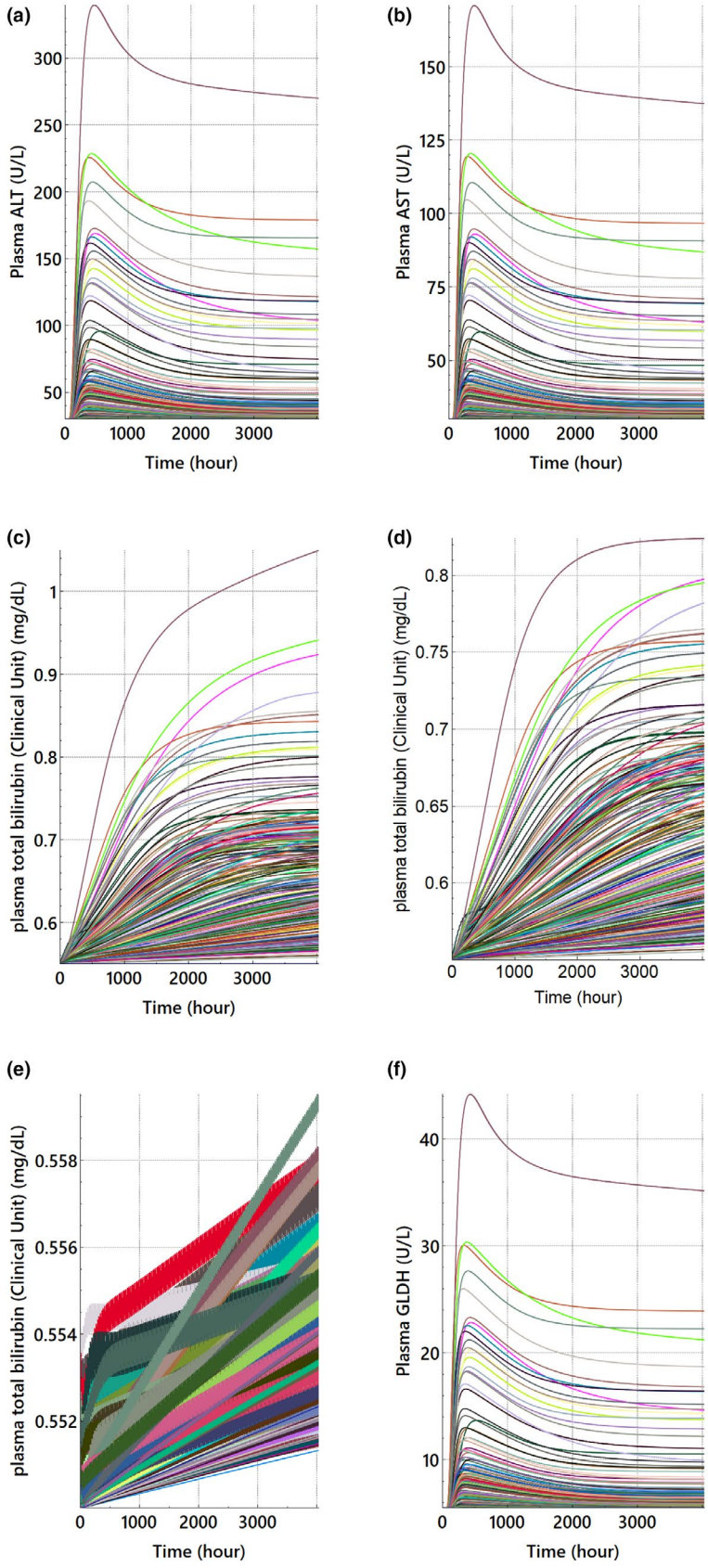

Figure 4 Predicted time course data for liver injury biomarkers: (**a**) ALT and (**b**) AST for ivacaftor and elexacaftor administered in combination; total plasma bilirubin for (**c**) ivacaftor and elexacaftor administered in combination, (**d**) ivacaftor alone, and (**e**) elexacaftor alone; (**f**) glutamate dehydrogenase (GLDH) for ivacaftor and elexacaftor administered in combination ($n = 285$ for all simulations, full dose for each compound).

following the same trend of a peak around 500 hours and decreasing over time (**Figure 4b**). In contrast, the predicted plasma total bilirubin levels for ivacaftor alone and ivacaftor with elexacaftor simulations rose steadily from 0.55 mg/dL and plateaued at 0.8–1 mg/dL near the ULN, while bilirubin levels for elexacaftor alone rose modestly from around 0.55 to 0.56 mg/dL (**Figure 4c,d**). In addition to ALT, AST, and bilirubin, elevations of emerging liver injury biomarkers such as glutamine dehydrogenase (GLDH) were also predicted. The predicted plasma levels of GLDH were lower than those of ALT or AST, but also aligned with the trend, peaking around 500 hours and slowly decreasing and plateauing afterward (**Figure 4f**).

In simulations of a 50% dose reduction of ETI or hypothetical antioxidant effects, a significant reduction in DILI occurrence was predicted for both therapeutic approaches. The 50% dose reduction simulation (elexacaftor 100 mg daily and ivacaftor 150 mg daily) resulted in a 0% (0/285) predicted occurrence of ALT elevations > 3× ULN or bilirubin > 2× ULN with a maximum ALT of 2.4× ULN (**Table 1**, **Figure 5a**). The antioxidant simulation (halved ROS production rate constant 1, halved ROS production rate Vmax 4) also resulted in a 0% (0/285) predicted occurrence of ALT elevations > 3× ULN or bilirubin > 2× ULN, but had a slightly lower maximum ALT of 2.2× ULN (**Table 1**, **Figure 5b**). In comparison, a full dose of ETI had a 6.0% (17/285) predicted occurrence of ALT elevations > 3× ULN or bilirubin > 2× ULN with a maximum ALT of 8.5× ULN (**Table 1**, **Figure 5c**). Thus, both a 50% dose reduction of ETI and the hypothetical antioxidant effect were predicted to have roughly the same impact on reducing ALT elevations below 3× ULN for all individuals in the $n = 285$ SimPops.

DISCUSSION

ETI is a highly effective modulator therapy for cystic fibrosis; however, clinical trials, case reports, and a pharmacovigilance analysis of real-world adverse event data have shed light on the risk of DILI associated with ETI.[3–12] This study uncovered the previously unknown mechanisms of hepatotoxicity due to ETI through *in vitro* assays and assessed the relative contribution of each mechanism and each ETI compound to DILI using in silico quantitative systems toxicology modeling. Additionally, the in silico modeling predicted the impact of therapeutic modifications of half-dose ETI and antioxidant administration on transaminase levels.

The *in vitro* results in HepG2 cells revealed that ivacaftor was the most significant driver of hepatotoxicity through the mechanisms of oxidative stress and mitochondrial dysfunction. For those mechanisms, ivacaftor caused toxicity within its predicted physiological concentration range and with higher potency than the positive controls, ciglitazone and troglitazone. For BSEP inhibition, elexacaftor was the most potent of the three ETI compounds; however, the concentrations needed for BSEP transport inhibition exceeded its predicted C_{max} in plasma and liver. Thus, across the three components of ETI, ivacaftor was the strongest *in vitro* contributor to hepatotoxicity through oxidative stress and mitochondrial dysfunction, with elexacaftor playing a secondary role as a mild BSEP inhibitor. The contribution of ETI metabolites to hepatotoxicity was also relatively minor in comparison to that of ivacaftor.

Mechanistic modeling performed in DILIsym confirmed that ROS production due to ivacaftor was the primary driver of LFT elevations due to ETI, while ETC inhibition and BSEP inhibition had a relatively negligible effect. Accordingly, therapeutics with ROS-scavenging and/or antioxidant activity could be ideal for counteracting DILI due to ETI. While the DILIsym predictions matched our *in vitro* observations that the oxidative stress due to ivacaftor was a major contributor to hepatotoxicity, they did not align with the fact that mitochondrial dysfunction due to ivacaftor was also highly toxic *in vitro*. This discrepancy may be due to the fact that it was necessary to turn on mitochondrial biogenesis in the DILIsym model in order to avoid overprediction of ETI DILI (preliminary simulations using an $n = 32$ SimPops while omitting mitochondrial biogenesis resulted in predicted occurrences of 22/32 (68.8%) for ALT > 3× ULN, 9/32 (28.1%) for bilirubin > 2× ULN, 9/32 (28.1%) for Hy's Law cases, and 1/32 (3.1%) for deaths).

The DILIsym modeling results also recapitulated the relative compound toxicities from *in vitro* assays and approximated the observed occurrence of liver enzyme elevations from clinical trials. Simulations of ivacaftor alone predicted a 4.9% occurrence of ALT elevations > 3× ULN, while simulations of elexacaftor alone predicted no ALT elevations > 3× ULN. Additionally, the simulations also revealed a synergistic toxic effect between ivacaftor and elexacaftor. Simulations of ivacaftor and elexacaftor combined predicted a 6.0% occurrence of ALT > 3× ULN, similar to the 8% published occurrence of ALT elevations > 3× ULN from the pivotal Phase III clinical trial for ETI.[3]

Furthermore, the time course of ALT elevations closely matched the onset time of DILI from our previous pharmacovigilance study of the association between ETI and DILI in the FAERS database. Peak plasma concentrations for ALT and AST in the simulations were reached at ~500 hours (21 days), which is close to the <2 month median onset time for DILI from our pharmacovigilance study and also aligns with new FDA guidance for LFT monitoring for ETI starting from 1 month after initiation.[12,15] This highlights that the predicted peak plasma LFT levels from QST modeling could be used to estimate the onset time for DILI for hepatotoxic compounds. Additionally, the nearly identical *in vitro* toxicity profile of deutivacaftor when compared to ivacaftor suggests that the newest CFTR modulator, vanzacaftor/tezacaftor/deutivacaftor, may induce LFT elevations in a pattern similar to that of ETI. Because translation of *in vitro* toxicity to clinical DILI needs to account for clinical exposure, further simulations will be needed to confirm that the hepatic concentration of deutivacaftor is comparable to that of ivacaftor.

Regarding emerging biomarkers of DILI, the simulated levels of GLDH tended to peak at the same time as ALT and AST but did not surpass ALT in magnitude, suggesting that GLDH does not offer an improvement over established biomarkers ALT and AST for detecting ETI-mediated DILI.

A limitation of the study was that LCMS analysis of cell lysate produced unreliable and low measurements of intracellular ETI; a possible cause could be that ETI has high binding to cell membrane proteins that impede full extraction of the compounds during sample processing for LCMS. Because there was no published data available to verify the results of the LCMS

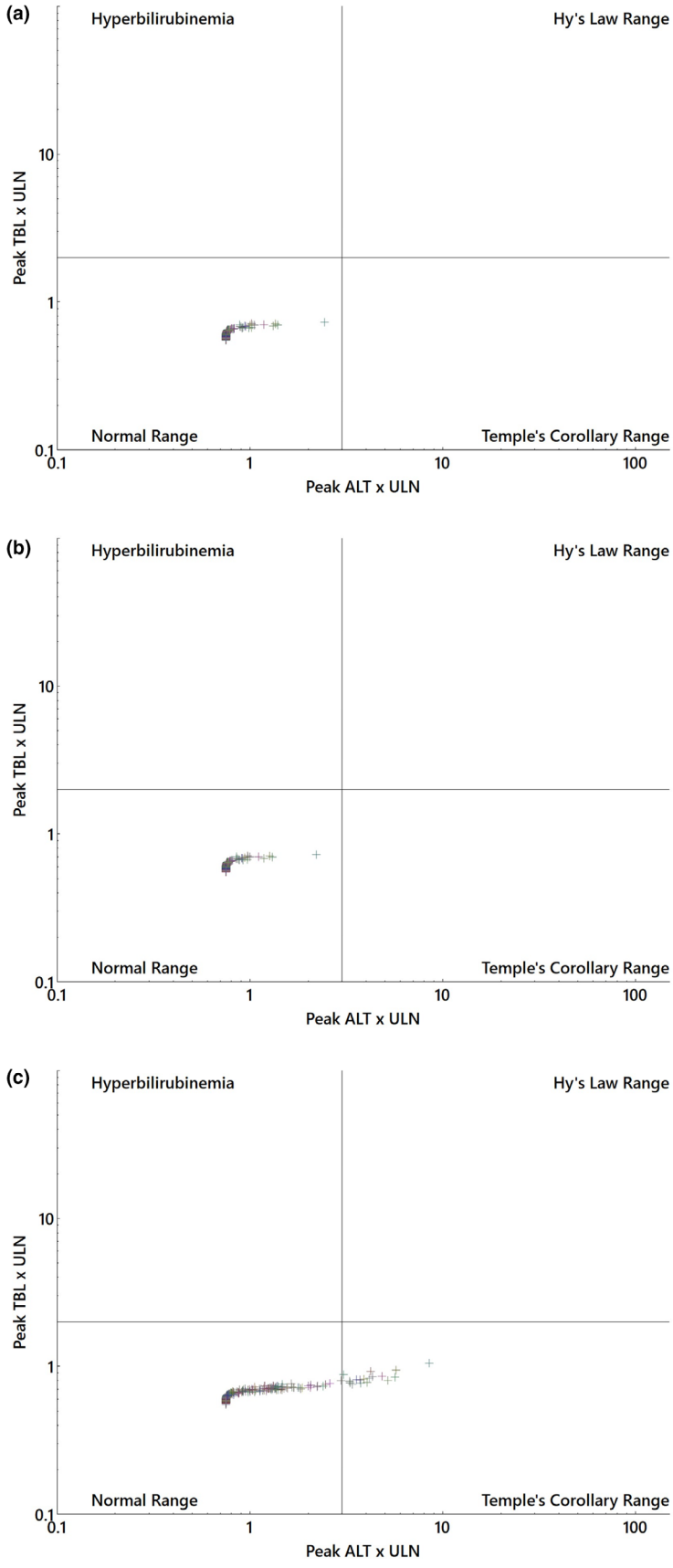

Figure 5 eDISH (evaluation of drug-induced serious hepatotoxicity) plots for simulations of (**a**) 50% dose reduction of ETI, (**b**) hypothetical antioxidant effects, and (**c**) full dose ETI. $n=285$ for all simulations.

Table 2 Sensitivity analysis for toxicity parameters

	Simulated ALT >3× ULN	Simulated bilirubin >2× ULN
Unchanged ROS and ETC Inhibition Parameters	1/32	0/32
0.25× parameters	0/32	0/32
0.5× parameters	0/32	0/32
2× parameters	10/32	1/32
4× parameters	27/32	12/32

measurements, the PBPK-derived liver:blood Kp value was used as an approximate conversion factor to calculate the intracellular ETI concentrations from the nominal concentrations. Since variation in intracellular concentrations is directly linked to toxicity parameterization in DILIsym, the uncertainty in modeled intracellular concentrations was addressed by conducting a sensitivity analysis on ROS and ETC inhibition toxicity parameters in DILIsym by varying the parameters in a range of 0.25×, 0.5×, 2×, and 4×, and running simulations in a small cohort ($n = 32$) of the built-in Human_ROS_apop_mito_BA_v8A_1 Simpops. The sensitivity analysis demonstrated that the tested parameter range captured outcomes both below and above the observed clinical incidence of ALT > 3× ULN (8%) in Phase III trials. The baseline (unchanged) parameters provided the closest approximation of the clinical outcome (**Table 2**). Overall, these findings indicate that hepatotoxicity predictions in DILIsym are sensitive to assumptions regarding intracellular concentrations. The current parameters, informed by in silico-estimated intracellular concentrations using a validated liver Kp, appear to reasonably replicate observed clinical hepatotoxicity outcomes, supporting their continued use.

A second limitation of DILIsym is that it was not designed to directly incorporate the effect of antioxidant coadministration. To conduct the simulations of antioxidant coadministration with ETI, a 50% reduction in both ivacaftor's ROS production rate constant 1 and elexacaftor's ROS production Vmax 4 was implemented to approximate the increase in GSH levels in the liver following administration of NAC in animals. A 25% reduction in the ROS parameters was also tested, resulting in a frequency of 3/285 for ALT > 3× ULN slightly higher than the effect of a 50% reduction (0/285 for ALT > 3× ULN).

Given our newfound knowledge of the mechanisms of ETI-mediated DILI, future studies exploring novel DILI biomarkers and for validating the predicted effect of therapeutic approaches (dose reduction and antioxidant treatment) are warranted.

SUPPORTING INFORMATION

Supplementary information accompanies this paper on the *Clinical Pharmacology & Therapeutics* website (www.cpt-journal.com).

ACKNOWLEDGMENTS

The authors would like to thank Christina Battista, Ph.D., of Simulations Plus Inc., for providing additional support for SimPops creation in DILIsym.

FUNDING

This work was supported by a grant from the Anton Yelchin Foundation.

CONFLICT OF INTEREST

K.Y. is an employee of DILIsym Services, a division of Simulations Plus, Inc. All other authors declared no competing interests for this work.

AUTHOR CONTRIBUTIONS

A.S., P.M.B., and K.Y. wrote the manuscript. A.S. and P.M.B. designed the research. A.S. and C.C. performed the research. A.S. and C.C. analyzed the data. K.Y. and P.M.B. contributed analytical tools.

1. Ong, T. & Ramsey, B.W. Cystic fibrosis: a review. *JAMA* **329**, 1859–1871 (2023).
2. Marshall, B. *et al*. *Patient Registry Annual Data Report* (Cystic Fibrosis Foundation, Bethesda, MD, 2021).
3. Middleton, P.G. *et al*. Elexacaftor-tezacaftor-ivacaftor for cystic fibrosis with a single Phe508del allele. *N. Engl. J. Med.* **381**, 1809–1819 (2019).
4. Heijerman, H.G.M. *et al*. Efficacy and safety of the elexacaftor plus tezacaftor plus ivacaftor combination regimen in people with cystic fibrosis homozygous for the F508del mutation: a double-blind, randomised, phase 3 trial. *Lancet* **394**, 1940–1948 (2019).
5. Sutharsan, S. *et al*. Efficacy and safety of elexacaftor plus tezacaftor plus ivacaftor versus tezacaftor plus ivacaftor in people with cystic fibrosis homozygous for F508del-CFTR: a 24-week, multicentre, randomised, double-blind, active-controlled, phase 3b trial. *Lancet Respir. Med.* **10**, 267–277 (2022).
6. Barry, P.J. *et al*. Triple therapy for cystic fibrosis. *N. Engl. J. Med.* **385**, 815–825 (2021).
7. Zemanick, E.T. *et al*. A phase 3 open-label study of elexacaftor/tezacaftor/ivacaftor in children 6 through 11 years of age with cystic fibrosis and at least one. *Am. J. Respir. Crit. Care Med.* **203**, 1522–1532 (2021).
8. Mall, M.A. *et al*. Efficacy and safety of elexacaftor/tezacaftor/ivacaftor in children 6 through 11 years of age with cystic fibrosis heterozygous for. *Am. J. Respir. Crit. Care Med.* **206**, 1361–1369 (2022).
9. Sharma, P. & Giddings, O.K. Acute Liver Failure in a Patient with Cystic Fibrosis Taking Triple Combination Modulator. Challenging Cases in Patients with Bronchiectasis. American Thoracic Society International Conference Abstracts: American Thoracic Society; p. A2113-A (2021).
10. Salehi, M., Iqbal, M., Dube, A., AlJoudeh, A. & Edenborough, F. Delayed hepatic necrosis in a cystic fibrosis patient taking elexacaftor/tezacaftor/ivacaftor (Kaftrio). *Respir. Med. Case. Rep.* **34**, 101553 (2021).
11. Smith, M. *et al*. Ivacaftor-elexacaftor-tezacaftor and tacrolimus combination in cystic fibrosis. *J. Cyst. Fibros.* **21**, e8–e10 (2022).
12. Shi, A., Nguyen, H., Kuo, C.B. & Beringer, P.M. Drug-induced liver injury associated with elexacaftor/tezacaftor/ivacaftor: a pharmacovigilance analysis of the FDA adverse event reporting system (FAERS). *J. Cyst. Fibros.* **23**, 566–572 (2024).
13. David, S. & Hamilton, J.P. Drug-induced liver injury. *US Gastroenterol. Hepatol. Rev.* **6**, 73–80 (2010).
14. Andrade, R.J. *et al*. Drug-induced liver injury. *Nat. Rev. Dis. Primers.* **5**, 58 (2019).
15. *Trikafta: Highlights of Prescribing Information* (Vertex Pharmaceuticals, Inc, Boston, MA, 2024).
16. Hoofnagle, J.H. & Knoben, J.E. Cystic Fibrosis Agents. In *LiverTox: Clinical and Research Information on Drug-Induced Liver Injury [Internet]* (National Institute of Diabetes and Digestive and Kidney Diseases, Bethesda, MD, 2021).

17. Bell, C.C. *et al*. Transcriptional, functional, and mechanistic comparisons of stem cell-derived hepatocytes, HepaRG cells, and three-dimensional human hepatocyte spheroids as predictive in vitro systems for drug-induced liver injury. *Drug Metab. Dispos.* **45**, 419–429 (2017).
18. Ramaiahgari, S.C., Waidyanatha, S., Dixon, D., DeVito, M.J., Paules, R.S. & Ferguson, S.S. Three-dimensional (3D) HepaRG spheroid model with physiologically relevant xenobiotic metabolism competence and hepatocyte functionality for liver toxicity screening. *Toxicol. Sci.* **160**, 189–190 (2017).
19. Longo, D.M., Shoda, L.K.M., Howell, B.A., Coric, V., Berman, R.M. & Qureshi, I.A. Assessing effects of BHV-0223 40 mg Zydis sublingual formulation and Riluzole 50 mg oral tablet on liver function test parameters utilizing DILIsym. *Toxicol. Sci.* **175**, 292–300 (2020).
20. Woodhead, J.L. *et al*. Analyzing the mechanisms behind macrolide antibiotic-induced liver injury using quantitative systems toxicology modeling. *Pharm. Res.* **36**, 48 (2019).
21. Shoda, L.K., Battista, C., Siler, S.Q., Pisetsky, D.S., Watkins, P.B. & Howell, B.A. Mechanistic modelling of drug-induced liver injury: investigating the role of innate immune responses. *Gene Regul. Syst. Biol.* **11**, 1177625017696074 (2017).
22. Woodhead, J.L., Watkins, P.B., Howell, B.A., Siler, S.Q. & Shoda, L.K.M. The role of quantitative systems pharmacology modeling in the prediction and explanation of idiosyncratic drug-induced liver injury. *Drug Metab. Pharmacokinet.* **32**, 40–45 (2017).
23. Woodhead, J.L. *et al*. Application of a mechanistic model to evaluate putative mechanisms of tolvaptan drug-induced liver injury and identify patient susceptibility factors. *Toxicol. Sci.* **155**, 61–74 (2017).
24. Smith, B. *et al*. Mechanistic investigations support liver safety of ubrogepant. *Toxicol. Sci.* **177**, 84–93 (2020).
25. Yang, K., Battista, C., Woodhead, J.L. & Watkins, P.B. Quantitative systems toxicology modeling using DILIsym suggests that drug-induced liver injury can be enhanced by co-administered drugs and mitigated by mitochondrial biogenesis AAPS Annual Meeting PharmSci 360; Ernest N. Morial Convention Center, New Orleans, LA, United States, America, (2020).
26. Woodhead, J.L. *et al*. Prediction of the liver safety profile of a first-in-class myeloperoxidase inhibitor using quantitative systems toxicology modeling. *Xenobiotica* **54**, 401–410 (2024).
27. Yang, K. *et al*. Quantitative systems toxicology modeling informed safe dose selection of emvododstat in acute myeloid leukemia patients. *Clin. Pharmacol. Ther.* **115**, 525–534 (2024).
28. Woodhead, J.L., Siler, S.Q., Howell, B.A., Watkins, P.B. & Conway, C. Comparing the liver safety profiles of 4 next-generation CGRP receptor antagonists to the hepatotoxic CGRP inhibitor telcagepant using quantitative systems toxicology modeling. *Toxicol. Sci.* **188**, 108–116 (2022).
29. *Alyftrek: Highlights of Prescribing Information* (Vertex Pharmaceuticals, Inc, Boston, MA, 2024).
30. Hong, E., Almond, L.M., Chung, P.S., Rao, A.P. & Beringer, P.M. Physiologically-based pharmacokinetic-led guidance for patients with cystic fibrosis taking elexacaftor-tezacaftor-ivacaftor with nirmatrelvir-ritonavir for the treatment of COVID-19. *Clin. Pharmacol. Ther.* **111**, 1324–1333 (2022).
31. Viswanathan, L. *et al*. Phase 1 study to assess the safety and pharmacokinetics of elexacaftor/tezacaftor/ivacaftor in subjects without cystic fibrosis with moderate hepatic impairment. *Eur. J. Drug Metab. Pharmacokinet.* **47**, 817–825 (2022).
32. *Extract From the Clinical Evaluation Report for Lumacaftor/Ivacaftor* (Therapeutic Goods Administration, Australia, 2015).
33. Agilent Technologies, Inc. *Agilent Seahorse XF Cell Mito Stress Test Kit User Guide* 3rd edn. (Agilent Technologies, Inc., Wilmington, DE, 2024).
34. Nadanaciva, S. *et al*. Assessment of drug-induced mitochondrial dysfunction via altered cellular respiration and acidification measured in a 96-well platform. *J. Bioenerg. Biomembr.* **44**, 421–437 (2012).
35. Longo, D.M., Yang, Y., Watkins, P.B., Howell, B.A. & Siler, S.Q. Elucidating differences in the hepatotoxic potential of tolcapone and entacapone with DILIsym(®), a mechanistic model of drug-induced liver injury. *CPT Pharmacometrics Syst. Pharmacol.* **5**, 31–39 (2016).
36. Liao, X., Wang, Y. & Wong, C.W. Troglitazone induces cytotoxicity in part by promoting the degradation of peroxisome proliferator-activated receptor γ co-activator-1α protein. *Br. J. Pharmacol.* **161**, 771–781 (2010).
37. Howell, B.A. *et al*. In vitro to in vivo extrapolation and species response comparisons for drug-induced liver injury (DILI) using DILIsym™: a mechanistic, mathematical model of DILI. *J. Pharmacokinet. Pharmacodyn.* **39**, 527–541 (2012).
38. Yang, Y. *et al*. MITOsym®: a mechanistic, mathematical model of hepatocellular respiration and bioenergetics. *Pharm. Res.* **32**, 1975–1992 (2015).
39. Popov, L.D. Mitochondrial biogenesis: an update. *J. Cell. Mol. Med.* **24**, 4892–4899 (2020).
40. Lakhani, V.V., Generaux, G., Howell, B.A., Longo, D.M. & Watkins, P.B. Assessing liver effects of cannabidiol and valproate alone and in combination using quantitative systems toxicology. *Clin. Pharmacol. Ther.* **114**, 1006–1014 (2023).
41. Arfsten, D.P., Johnson, E.W., Wilfong, E.R., Jung, A.E. & Bobb, A.J. Distribution of radio-labeled N-acetyl-L-cysteine in Sprague-Dawley rats and its effect on glutathione metabolism following single and repeat dosing by oral gavage. *Cutan. Ocul. Toxicol.* **26**, 113–134 (2007).
42. Knight, T.R., Ho, Y.S., Farhood, A. & Jaeschke, H. Peroxynitrite is a critical mediator of acetaminophen hepatotoxicity in murine livers: protection by glutathione. *J. Pharmacol. Exp. Ther.* **303**, 468–475 (2002).